Oxygen Reduction at Platinum Monolayer Islands Deposited on Au(111)

Anusorn Kongkanand and Susumu Kuwabata*

Department of Applied Chemistry, Graduate School of Engineering, Osaka University, Suita, Osaka 565-0871, Japan

Received: June 15, 2005; In Final Form: October 18, 2005

Atomic monolayer islands of Pt, namely, two-dimensional Pt nanoparticles, on a Au(111) electrode have been studied for the first time, focusing on their electrocatalytic activities for oxygen reduction in acid solutions. The Pt islands' electrodes were prepared using the self-assembled technique of thiols together with the replacement of Pt with a Cu monolayer. The states of adsorbed OH and the catalytic activities of oxygen reduction were sensitive to the Pt island size. As island size decreased, a delay in the reduction of surface oxide was observed. However, negligible influence of adsorbed OH on activity for oxygen reduction was observed. Pt islands of sizes ranging from 5 to 10 nm showed higher specific catalytic activities for oxygen reduction. Specific catalytic activities decreased by a factor of 10 with a decrease in island sizes from 5.5 to 3.1 nm. Size effects observed in Pt monolayer islands were discussed in comparison with three-dimensional nanoparticles, to obtain information concerning the size effects of metal nanoparticles.

1. Introduction

Metal nanoparticles are attracting great scientific interest as a result of their novel properties compared with those of bulk materials.[1] These are ascribable to electronic as well as geometric factors. Several studies have been conducted for decades in order to clarify the relationship between particle size and its catalytic activities.[2−8] However, difficulty in preparing metal nanoparticles having uniform quality with fewer lattice defects and small size distribution is a reason contradicting results were obtained among research groups.[9] Such complicated parameters could be excluded if two-dimensional materials were utilized. Remarkable success has been achieved by Goodman et al. in a study on Au nanoparticles on titania with scanning tunneling spectroscopy, by which electronic changes related to the quantum size effect were found to appear in Au particles smaller than 3.5 nm in diameter and three atomic layers in height.[10−13]

Pt is known to be the best electrocatalyst for oxygen reduction in acid fuel cells. Pt nanoparticles are generally deposited on conductive support to use them efficiently as catalysts. From a viewpoint of heterogeneous catalytic reaction, the optimum use of the metal can be achieved by using two-dimensional nanoparticles, all metal atoms of which are exposed to the reactant. However, real two-dimensional nanoparticles possessing long-term stability are not easy to prepare.

It has been found in our previous study[14] that underpotential deposition (UPD) of several kinds of metals can be made even on a gold electrode coated with a self-assembled monolayer of alkanethiol. In the initial stage of the deposition, numerous islands of metal atomic monolayer are generated, and they grow gradually with polarization time, allowing the preparation of monolayer islands having the desired size on a Au substrate.[15,16] Electrochemical properties of the metal monolayer islands can be investigated after removing the adsorbed thiol molecules by electrochemical means. For the first demonstration on electrocatalytic analysis of the metal monolayer islands, we investigated oxygen reduction on Ag monolayer islands deposited on a Au electrode having a quasi-(111) crystal face. It has been, then, found that there is a threshold value in the island size against oxygen reduction with the four-electron reaction.[17] After several electrochemical manipulations and oxygen reduction for ca. 2 h, electrochemical characterization using voltammetry and scanning tunneling microscopic (STM) images of the electrodes showed no significant changes in size, shape, or coverage of the islands, reflecting their high stability as electrocatalysts.

SCHEME 1: Schematic Illustration of Procedures for Preparing Pt Monolayer Islands

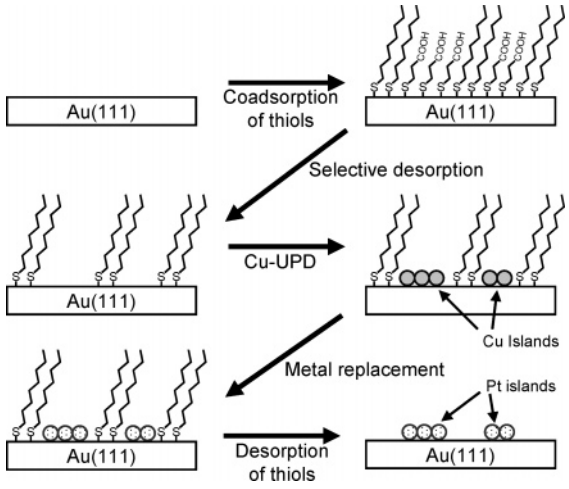

In cases of noble metals including Pt, of which ions do not exhibit UPD behavior, metal monolayer islands can be prepared by combining the following techniques: self-assembled monolayer technique of thiols, UPD, and replacement deposition of noble metals.[18] Binary thiols were coadsorbed on Au (Scheme 1), followed by the selective desorption of one thiol component to form nanopores in the membrane.[19] Cu monolayers are deposited at the nanopores by UPD. Then, dipping the resulting electrode in a solution containing noble metal ions induces the

* Corresponding author phone: 81-6-6879-7372; fax: 81-6-6879-7372; e-mail: kuwabata@chem.eng.osaka-u.ac.jp.

10.1021/jp053229f CCC: $30.25
Published on Web 11/17/2005

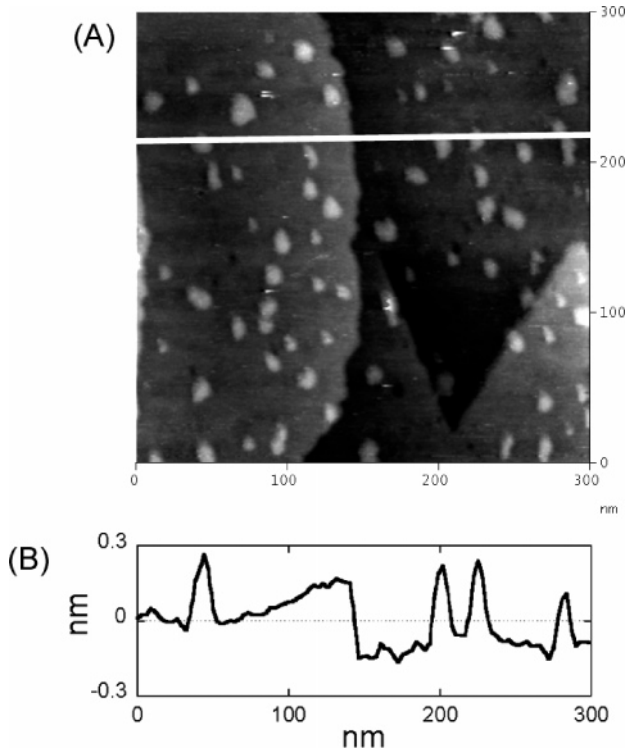

Figure 1. (A) STM image (300 × 300 nm^2) of Pt monolayer islands after desorption of thiols. The image was obtained with a bias voltage of 0.2 V and a tip current of 1 nA in the air. A cross-sectional profile (B) was taken along the white line. The mean island size was 8.6 nm.

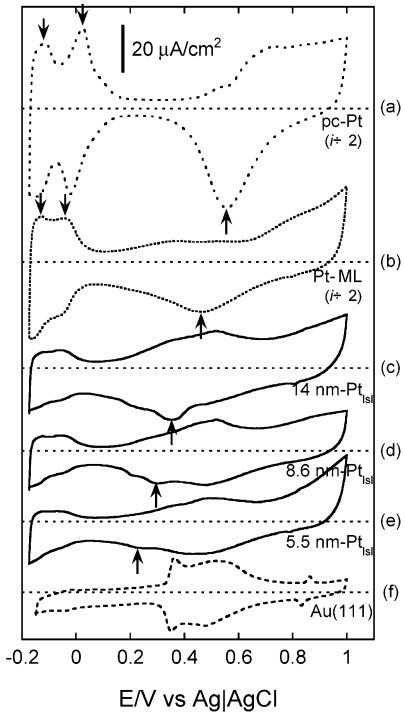

Figure 2. Cyclic voltammetry curves for polycrystalline Pt (a); Pt ML (b); Pt islands of island sizes of 14 nm (c), 8.6 nm (d), and 5.5 nm (e); and Au(111) (f) electrodes obtained in N_2-saturated 0.1 M sulfuric acid at a scan rate of 50 mV/s. Black and gray arrows in the figure indicate current peaks of surface oxide reduction and oxidative hydrogen desorption, respectively.

replacement of the noble metal with a Cu monolayer,[20] giving noble metal monolayer islands.[18] A typical STM image of the electrode prepared with this method is shown in Figure 1. Comparable stability as an electrocatalyst to Ag monolayer islands was also found for Pt monolayer islands. The present paper describes oxygen reduction on Pt monolayer islands in acid solutions together with the effect of OH adsorption on Pt islands on oxygen reduction.

2. Experimental Section

Gold having a quasi-(111) surface used in this study was prepared by vacuum evaporation of Au on a freshly cleaved natural mica sheet (Nilaco) at 290 °C. All solutions were made using water purified by a Millipore Milli-Q Gradient A10 system. All chemicals were of reagent grade and were used without any specific purification.

The preparation of the Pt monolayer island electrode was fully described in our previous paper.[18] Briefly, a clean Au(111) substrate was immersed into an ethanol solution containing a given concentration of 1-octanethiol (OT) and 3-mercaptopropionic acid (MPA) for 1 h to form a binary self-assembled monolayer of the thiols. The electrode was then rinsed with water and moved to an electrochemical cell containing 0.5 M KOH. Polarization of the electrode at −0.60 V versus Ag/AgCl for 10 min selectively removed MPA, forming nanometer-scale pores in the remaining OT monolayer. UPD of Cu was made at the nanopores; then, the Cu monolayer islands were brought into contact with a deoxygenated solution of 1 mM K_2PtCl_4 + 0.1 M H_2SO_4 for 3 min, inducing the replacement of Cu islands with Pt islands. Then, all adsorbed thiols were eliminated by polarizing at −1.5 V versus Ag/AgCl in a 0.5 M KOH solution. This will be denoted as a Pt island electrode. In addition, changing the concentration ratio of MPA and OT can vary the mean size of Pt islands ranging from 3 to 14 nm. The Pt coverage on the prepared electrode was estimated by STM observations together with by voltammetry for the reduction of Au oxide in perchloric acid.[21,22]

Electrochemical measurements were carried out using a three-electrode cell with a Pt foil serving as a counterelectrode and $Ag/AgCl/KCl_{sat}$ serving as a reference electrode. All potentials cited here are those relative to this reference electrode. A glass tube with open ends was used as an electrochemical cell. The reference electrode was connected to the electrochemical cell with a double-junction electrolyte to prevent chloride contamination. The Au substrate was attached at the bottom hole of the cell with a Teflon-coated O-ring to give an active electrode area of 0.32 ± 0.02 cm^2, which was estimated by measuring the charges involved in the oxidation of chemically adsorbed iodine. STM observations were preformed in air using a Nanoscope III STM apparatus (Digital Instruments, Inc.).

3. Results and Discussion

3.1. Cyclic Voltammetry of Pt Monolayer Islands in a Sulfuric Acid Solution. Oxygen reduction on Pt has been known to show pronounced sensitivities against its surface structure, that is, its crystalline profile; adsorption of oxide species (OH_{ads}); and anions from supporting electrolytes.[23−28] The as-prepared Pt monolayer appeared to be covered with adsorbed chloride from the precursory tetrachloroplatinate. Thus, it is necessary to refresh the surface by cycling the electrode potential between −0.175 and 1.0 V for several cycles prior to characterization. The stationary cyclic voltammograms after repeated potential cycles for the Pt monolayer (Pt ML) and Pt monolayer islands (Pt islands) taken in a sulfuric acid solution are shown in Figure 2. The coverages of Pt on the electrodes are summarized in Table 1. The voltammogram obtained for the Pt ML (Figure 2b) was similar to that for polycrystalline Pt

TABLE 1. Characterizations of Pt Islands and the Pt ML and Some of Their Kinetics Parameters for Oxygen Reduction

	MPA/OT	island size[a] (nm)	island density (μm^{-2})	Pt coverage[b] (%)	Tafel slope (mV dec^{-1})	current density at 0.55 V[b] [$\log(i_{0.55})$/A cm^{-2} − Pt]
Pt islands	2.0	3.1 ± 0.41	3440	2.6 ± 0.6	112	−4.85 ± 0.13
	2.25	4.4 ± 0.52	2370	3.6 ± 0.8	109	−4.17 ± 0.11
	2.5	5.5 ± 0.73	2000	4.8 ± 1.0	100	−3.86 ± 0.10
	3.25	8.6 ± 0.87	1380	8.0 ± 1.5	96	−3.92 ± 0.10
	4.0	10.9 ± 1.6	1250	11.7 ± 1.9	94	−4.11 ± 0.09
	5.0	14.0 ± 2.8	1090	16.8 ± 2.7	93	−4.19 ± 0.08
Pt ML				70 ± 6.0	86	−4.16 ± 0.07

[a] Deviations show a size distribution of >95% of the islands in the electrode estimated by STM. [b] Deviations show values ranging among electrodes prepared with a given condition.

(Figure 2a). Note that metal is known to reconstruct its surface structure when surface oxides are formed, and the crystalline profile of the surface changes after potential cycling up to 1.0 V.[29] Accordingly, we were unable to determine the crystalline profile of the as-prepared Pt monolayer from the voltammogram taken after the previous potential cycles.

The STM observation of the Pt ML was in agreement with that made by Sasaki et al.[30] Pt coverage of the electrode was estimated to be ca. 0.7. When the Pt ML is compared with polycrystalline Pt, the onset potential of surface oxide formation on the Pt ML shifted toward a higher potential (from 0.57 V for polycrystalline Pt to 0.66 V for the Pt ML), and the peak potential of oxide reduction on the Pt ML shifted toward a lower potential (from 0.55 V for polycrystalline Pt to 0.46 V for the Pt ML). The coverage of OH_{ads} on the Pt ML appeared to be lower than that on polycrystalline Pt. The oxide reduction wave was so broad that it extended into the potential region where the polycrystalline Pt exhibited only double-layer capacitance. These observations indicated a higher irreversibility of adsorption and desorption of OH on the Pt ML. A similar tendency was also observed on a Ti-supported thin Pt film, when its film thickness decreased to below 5 nm.[31] Two main peaks at +0.02 V and −0.11 V typically observed for polycrystalline Pt in the hydrogen adsorption region were observed on the Pt ML with a small shift to a more negative potential (at −0.04 V and −0.13 V), indicating a lower adsorption energy of hydrogen at the Pt ML.

Since the surface of Au(111) and the Pt monolayer at the Pt island electrode must be exposed to the electrolyte, features from both surfaces were expected. Cyclic voltammograms of Pt islands taken in sulfuric acid are shown in Figure 2c−e. Owing to very low Pt coverage in Pt island electrodes (see Table 1), the oxide reduction wave was rather small; however, it was still distinguishable. In Figure 3, the relationship between islands' sizes and their oxide reduction peak potentials is summarized. The distribution of the island sizes and the half-width of the reduction peaks are denoted as vertical and horizontal bars, respectively, in the figure. As the island size decreases, the oxide reduction wave shifted to a lower potential. It has been reported that the carbon-supported Pt (3D nanoparticles) exhibits a similar tendency[3−5] that is generally ascribed to an increased activation energy of adsorption of the oxygen intermediate at low coordination surface metal sites and a change in adsorbed oxide species from PtO to Pt_2O in very small particles.

Oxidative hydrogen desorption features in the hydrogen UPD region are generally used for characterizing the crystalline profile of Pt nanoparticles.[9] Kinoshita and Stonehart have concluded that two distinct anodic waves are associated with the ⟨111⟩ and ⟨100⟩ crystal faces and that a small wave appearing between the two waves is associated with adsorbed hydrogen on edge atoms of Pt nanoparticles.[32] As the size of Pt nanoparticles decreases, the latter wave becomes obvious while the wave assignable to hydrogen desorption from the ⟨100⟩ crystal face diminishes.[32,33] Considering that ⟨100⟩ is the dominant electrocatalytically active site on nanoparticles, a decrease in the ⟨100⟩ face is suggested to be the origin of activity loss in oxygen reduction observed for very small Pt nanoparticles (<4 nm).[2] Contrary to a variation of hydrogen peaks due to a change in the distribution of the crystalline profile on Pt particles, no significant change in the hydrogen peaks was seen on Pt islands, indicating that a decrease in island size does not induce a significant change in the crystalline profile. In addition, although the distributions of Pt atoms at the edge of the islands and Pt atoms inside the islands varied from 1:11 to 1:4 for 14 and 5.5 nm, by assuming that the islands have a Pt(111) structure, only two distinct anodic waves were seen. This fact suggested that the chemical properties of hydrogen adsorption on edge Pt atoms and that on inside Pt atoms are identical.

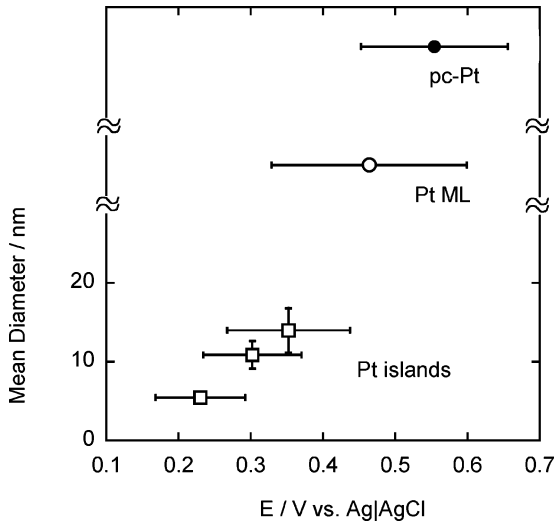

Figure 3. Reduction peak potential of oxide in Figure 2 as a function of island size. The distribution of the island sizes and the half-width of the reduction peaks are denoted as vertical and horizontal bars, respectively, in the figure.

3.2. Oxygen Reduction on the Pt Monolayer. Oxygen reduction of the Pt ML on Au(111) was first examined by Sasaki et al. using a rotating disk electrode in perchloric acid.[30] The overlayer Pt remarkably activated a poor electrocatalytic gold; however, it exhibited somewhat slower reaction kinetics than polycrystalline Pt. We obtained comparable results when observing a steady-state current in sulfuric acid, as shown in Figure 4. A shift to a lower potential by ca. 100 mV was found in the onset current for the Pt ML, as compared with polycrystalline Pt. A Tafel slope of about −86 mV/dec for oxygen reduction on the Pt ML at a low current density was observed. This is in contrast with polycrystalline and single-crystalline

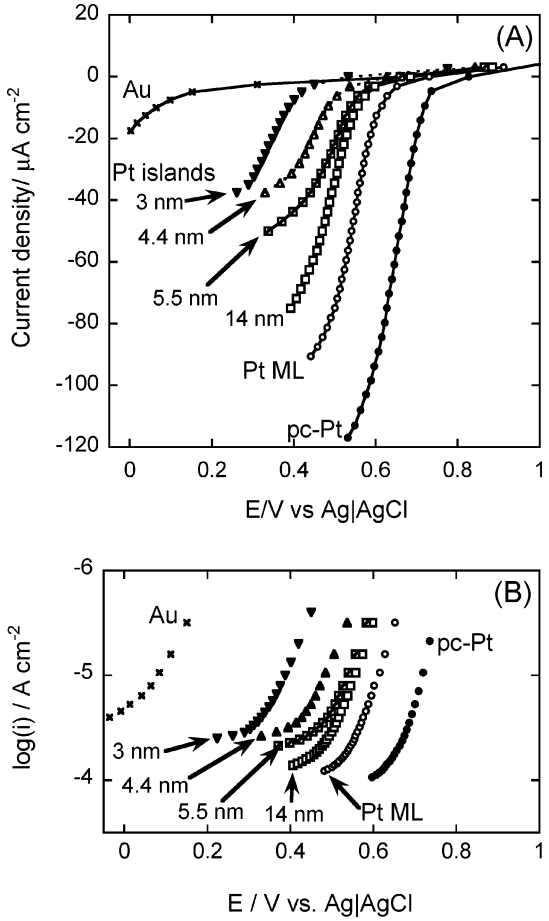

Figure 4. (A) Steady-state $i-E$ curves for oxygen reduction in O_2-saturated 0.1 M sulfuric acid at Au(111), polycrystalline Pt, Pt ML, and Pt islands with the mean island size as denoted in the figure. (B) The corresponding Tafel plots.

Pt, which usually show a slope of ca. −60 mV/dec at a low current density and a slope of ca. −120 mV/dec at a high current density.[34−39] It is believed that the change in the Tafel slope is reflected by potential-dependent changes in coverage of adsorbed OH on the Pt surfaces. Marković et al.[27] assumed that, in addition to site blocking, adsorbed OH alters the adsorption energy of oxygen on the electrode surface. Wang et al. demonstrated a model to quantitatively evaluate the effect of OH_{ads} on oxygen reduction.[40] The model, which was derived from the Butler−Volmer equation, allows a quantitative evaluation of geometric site-blocking effects and electronic effects as a function of OH_{ads} coverage (see eq 7 in ref 40). It is assumable from the model that, with increasing overpotential, the above-mentioned effects are reduced in the potential region where OH_{ads} coverage is decreasing (oxide reduction region), resulting in an enhancement of oxygen reduction currents. Hence, the apparent Tafel slope is smaller than that (−120 mV/dec) obtained in the potential region where no OH_{ads} exists on the electrode surface. As mentioned above, in the case of the single crystalline Pt, the effects by OH_{ads} give a Tafel slope of −60 mV/dec. However, relatively high Tafel slopes of −74 to −90 mV/dec were obtained for the Pt ML on Pd(111)[41] and Pt skin on Pt_3Ni or Pt_3Co,[42] which were found to have low OH_{ads} coverage. It is suggested that our Pt ML exhibiting a Tafel slope of −86 mV/dec also has low OH_{ads} coverage as compared to that of the crystalline Pt.

Shifts to lower potentials by ca. 100 mV in the onset potential of O_2 reduction as well as surface oxide reduction at the Pt ML are ascribable to an electronic effect from the underlying Au.

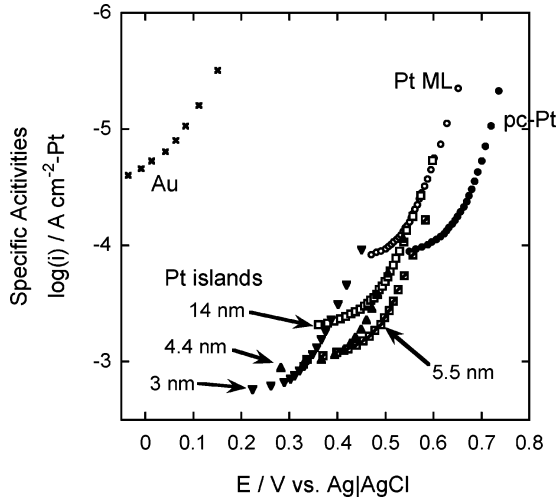

Figure 5. Tafel plots for Pt ML and Pt island electrodes for oxygen reduction in sulfuric acid, where current density was evaluated using the real surface area of Pt.

Underlying noble Au was expected to shift the d-band center of the Pt overlayer to a higher state. A shift of about 0.2 eV was found for a Pt−Au alloy,[43] and about 0.43 eV was calculated for a pseudomorphic Pt ML on Au(111).[44] The shift of the d-band center to a higher state should lower the 5d vacancy in the Pt ML, thus leading to a contracted 2π electron donation from the oxygen molecule to Pt. As a result, oxygen adsorption on the surface decreased, lowering the kinetic of oxygen reduction. This could be considered as an opposite case with an alloy of Pt and less-noble metals, which enhances d-band vacancies and facilitates oxygen reduction.[37,42,45−47]

3.3. Oxygen Reduction on Pt Monolayer Islands. As described previously, there is a delay in reduction of the surface oxide species on the Pt ML, and the delay is enhanced with a decrease in Pt island size. Small Pt islands, therefore, can be considered as unfavorable catalysts for oxygen reduction. However, as shown in Figures 3 and 4, the degree of negative shifts of the onset potential for oxygen reduction is obviously smaller than the potential shift observed for the oxide reduction. The dominant cause of the shift in oxygen reduction is probably due to the difference in absolute Pt area on the electrode. To determine the kinetics of Pt islands, the actual Pt area was estimated from the Pt coverage for each Pt island electrode, and then, their Tafel plots based on the obtained value were derived, and these are shown in Figure 5. Compared to the shifts in surface oxide reduction, shifts in oxygen reduction are apparently very small, implying that adsorbed OH has a small influence on oxygen reduction on the Pt ML, in comparison with polycrystalline or single-crystalline Pt.

Table 1 summarizes the characterizations of the islands and some of their kinetic parameters for oxygen reduction. The Tafel slopes tended to increase as the island size decreased. This is consistent with results obtained by Takasu et al. using Pt deposited on glassy carbon.[4] As already mentioned above, the model[40] proposed by Wang et al. predicts that as oxygen reduction in the potential region where OH_{ads} coverage decreases (oxide reduction region), the Tafel slope drops from −120 mV/dec to a lower value, by a certain magnitude depending on the OH_{ads} coverage. The observed increase in the Tafel slope with a decrease in island size seems to be related to the phenomenon that the degree of negative shift of OH_{ads} reduction with decreasing island size is larger than that of the onset potential of O_2 reduction. For example, the Pt ML electrode exhibits the straight Tafel slope at potentials ranging from 0.63 to 0.55 V

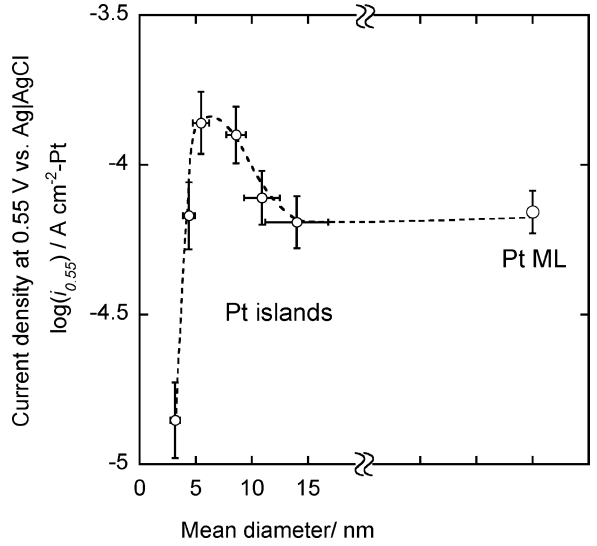

Figure 6. Specific catalytic current density at 0.55 V vs Ag/AgCl in Figure 5 as a function of mean Pt island size. The distribution of the island sizes and the deviation of catalytic currents are denoted as horizontal and vertical bars, respectively, in the figure.

where the reduction of OH_{ads} proceeds as shown in Figure 3, whereas the reduction of OH_{ads} on the 5.5 nm islands takes place at potentials ranging from 0.29 to 0.16 V that are much lower than the potential region where the Tafel straight line appears (0.58−0.50 V). The capability of surfaces of the Pt islands for O_2 reduction even in the presence of OH_{ads} is probably due to a low coverage of OH_{ads}.

The catalytic currents at 0.55 V versus Ag/AgCl estimated from Figure 5 were plotted as a function of the mean diameter of Pt islands as shown in Figure 6. The distribution of the island sizes and the deviation of catalytic currents are denoted as horizontal and vertical bars, respectively, in the figure. It is worth noting that all Pt atoms in the Pt ML are exposed to the reactant, giving the situation that mass activity is equal to specific activity. The specific activity diminished rapidly when the island became smaller than 5 nm. In the case of highly dispersed Pt on carbon, it is known that the specific activity for oxygen reduction diminishes at very small particle sizes. Peuckert et al. found a decrease in activities by a factor of 20 as the Pt particle size decreased from 3 to 1 nm, provided that the optimum activity per unit weight of Pt is obtained between 3 and 5 nm.[3] The origin of the structure sensitivity is usually described as an increased strength of OH adsorption as the adsorbed oxide species change from PtO to Pt_2O or as a change in the surface crystalline structure.[9] In the scanning tunneling spectroscopy study on nanosize particles of noble metal evaporated to titania, Goodman et al. showed that a band gap, which is usually a nonmetallic property, appears if the size of the Au particle on titania is reduced to below 3.5 nm (3.5 nm in diameter and 1.0 nm in height, ca. 300 atoms per particle).[10−13] It has been, then, considered that such an electronic change is responsible for the very high activity of Au nanoparticles toward CO oxidation at low temperatures.

Figure 6 shows that the smallest size of a Pt island exhibiting sufficient catalytic activities is ca. 5 nm. The optimum size for carbon-supported Pt particles was reported to vary from 2 to 4 nm depending on the carbon supports, catalyst exposure, catalyst preparation, and so forth. Although there are differences in size and shape, it is worth noting that a 2 nm Pt particle and a 5 nm Pt island contain almost the same number of Pt atoms (275 ± 63).

Specific activities of oxygen reduction on Pt islands of a mean diameter between 5 and 10 nm tended to be higher than that on the Pt ML. This peculiar behavior would be related to electronic factor, island edge density, or any contribution made by the Au surface including the migration of intermediates between Au and Pt islands. Further speculation awaits a detailed characterization of the electrode surface during oxygen reduction.

The so-called particle size effect of metal nanoparticles is explained in different ways. The size effect on carbon-supported Pt particles is generally described as reducing an electrocatalytic-active crystal face at small particles.[2,3,9] Titania-supported Au particles exhibited band gaps, which are related to a quantum size effect, with respect to the thickness of Au particles.[11,12] In the case of Pt monolayer islands, where no obvious change in the crystalline profile is observed, electronic property change is more likely. It is interesting to note that a 5 nm Pt island, which exhibits the highest catalytic activity for O_2 reduction, contains about the same number (ca. 300 atoms) of metal atoms as the titania-supported noble metal island, which exhibits a band gap, though there are differences in shape, dimension, and kinds of metals. In addition to this fact, in the case of even Pt particles, as already mentioned above, ca. 300 atoms is the minimum number for exhibiting the catalytic activities, suggesting strongly that the number of atoms is the main factor for determining the electronic property of the metal that influences its catalytic activities. A characterization of Pt islands including computer simulation is to be done to explore the electronic properties of Pt monolayer islands.

In Figure 5, it is also noteworthy that the limiting current density increases as the island size decreases. Oxygen reduction on the Pt island electrode, which can be considered as an array of ultramicroelectrodes (UMEs), should develop spherical diffusion on each Pt island. The steady-state current i_{ss} at a Pt island, when assuming as a disklike UME, can be described as

$$i_{ss} = \frac{4nFAD_O C_O^*}{\pi r_0}$$

where r_0 is radius of the island and n, F, A, D_O, and C_O* have their usual significance. This explains the increase in limiting current densities as the island size decreases.[48] In addition, on a spherical electrode in the absence of convective flow, the diffusion layer thickness, δ, can be expressed in terms of the electrode radius r_0 (e.g., $\delta = ar_0$, where a is a numerical constant).[48,49] If this is still effective at the nanoscale, where the size of the electric double layer is not negligible, one could expect less magnitude of the overlap of the spherical diffusion layer on small Pt islands, which allows higher limiting current densities and optimum utilization of the Pt electrocatalyst. The increase in limiting current density observed here is evidence of Pt islands behaving as an array of UMEs, even when their sizes are as small as 3 nm.

4. Conclusion

Pt monolayer islands deposited on Au(111) were first studied on oxygen reduction. Their catalytic activities for oxygen reduction and their surface oxide reduction have been discussed in comparison with three-dimensional nanoparticles, to give information concerning the size effects of nanoparticles. Pt islands, which were prepared using the self-assembled technique of thiols and the replacement of Pt with a Cu monolayer, exhibited special catalytic activities for oxygen reduction. Cyclic

voltammetry on Pt islands showed that there was a negative shift in reduction of the surface oxide and the shift increased with a decrease in island size. Further observations using a steady-state current showed that adsorbed OH has no obvious influence on oxygen reduction, reflecting a different state and coverage of adsorbed OH on the Pt islands. Oxygen appeared to be reduced on the Pt ML and Pt islands through a mechanism essentially similar to that of polycrystalline Pt. A relatively lower reaction rate of oxygen reduction on the Pt ML compared to that of polycrystalline Pt was due to the electronic effect from the underlying Au.

Oxygen reduction is sensitive to the size of the Pt islands. Pt islands in a region of 5−10 nm showed even higher specific activities than those of the Pt ML. The specific activity diminished rapidly when the island was reduced to below 5 nm. A change in electronic properties is probably responsible for the size sensibility in Pt islands. The specific reaction rate for oxygen reduction on Pt islands is lower than that on carbon-supported Pt nanoparticles and polycrystalline Pt. However, the very low Pt loading and the behavior against the surface oxide of the islands at high potentials still make them attractive as novel nanostructured electrocatalysts.

Acknowledgment. This work is partially supported by CREST of JST (Japan Science and Technology Corporation) and by New Energy and Industrial Technology Development Organization (NEDO) of Japan. A.K. expresses his thanks to the Center of Excellence (21COE) Program "Creation of Integrated EcoChemistry" of Osaka University.

References and Notes

(1) *Catalysis and Electrocatalysis at Nanoparticle Surfaces*; Wieckowski, A., Savinova, E. R., Vayenas, C. G., Eds.; Marcel Dekker: New York, 2003.

(2) Kinoshita, K. *J. Electrochem. Soc.* **1990**, *137*, 845.

(3) Peuckert, M.; Yoneda, T.; Betta, R. A. D.; Boudart, M. *J. Electrochem. Soc.* **1986**, *133*, 944.

(4) Takasu, Y.; Ohashi, N.; Zhang, X.-G.; Murakami, Y.; Minagawa, H.; Sato, S.; Yahikozawa, K. *Electrochim. Acta* **1996**, *41*, 2595.

(5) Maillard, F.; Eikerling, M.; Cherstiouk, O. V.; Schreier, S.; Savinova, E.; Stimming, U. *Faraday Discuss.* **2004**, *125*, 357.

(6) Henry, C. R. *Surf. Sci. Rep.* **1998**, *31*, 235.

(7) Watanabe, M.; Sei, H.; Stonehart, P. *J. Electroanal. Chem.* **1989**, *261*, 375.

(8) Heiz, U.; Sanchez, A.; Abbet, S.; Schneider, W.-D. *J. Am. Chem. Soc.* **1999**, *121*, 3214.

(9) Mukerjee, S. *J. Appl. Electrochem.* **1990**, *20*, 537.

(10) Xu, C.; Lai, X.; Zajac, W.; Goodman, D. W. *Phys. Rev. B: Condens. Matter Mater. Phys.* **1997**, *56*, 13464.

(11) Lai, X.; Clair, T. P. S.; Valden, M.; Goodman, D. W. *Prog. Surf. Sci.* **1998**, *59*, 25.

(12) Valden, M.; Lai, X.; Goodman, D. W. *Science* **1998**, *281*, 1647.

(13) Rainer, D. R.; Xu, C.; Goodman, D. W. *J. Mol. Catal. A* **1997**, *119*, 307.

(14) Oyamatsu, D.; Nishizawa, M.; Kuwabata, S.; Yoneyama, H. *Langmuir* **1998**, *14*, 3298.

(15) Oyamatsu, D.; Kuwabata, S.; Yoneyama, H. *J. Electroanal. Chem.* **1999**, *473*, 59.

(16) Oyamatsu, D.; Kanemoto, H.; Kuwabata, S.; Yoneyama, H. *J. Electroanal. Chem.* **2001**, *497*, 97.

(17) Kongkanand, A.; Kuwabata, S. *Electrochem. Commun.* **2003**, *5*, 133.

(18) Kongkanand, A.; Kuwabata, S. *Electrochemistry* **2004**, *72*, 412.

(19) Munakata, H.; Kuwabata, S.; Ohko, Y.; Yoneyama, H. *J. Electroanal. Chem.* **2001**, *496*, 29.

(20) Brankovic, S. R.; Wang, J. X.; Adžić, R. R. *Surf. Sci.* **2001**, *474*, L173.

(21) Hamelin, A. *J. Electroanal. Chem.* **1996**, *407*, 1.

(22) Angerstein-Kozlowska, H.; Conway, B. E.; Hamelin, A.; Stoicoviciu, L. *Electrochim. Acta* **1986**, *31*, 1051.

(23) Anderson, A. B. *Electrochim. Acta* **2002**, *47*, 3759.

(24) Abe, T.; Swain, G. M.; Sashikata, K.; Itaya, K. *J. Electroanal. Chem.* **1995**, *382*, 73.

(25) Hsieh, S.-J.; Gewirth, A. A. *Surf. Sci.* **2002**, *498*, 147.

(26) Stamenković, V.; Marković, N. M.; Ross, P. N. J. *J. Electroanal. Chem.* **2001**, *500*, 44.

(27) Marković, N. M.; Gasteiger, H. A.; Grgur, B. N.; Ross, P. N. *J. Electroanal. Chem.* **1999**, *467*, 157.

(28) Hsueh, K.-L.; Gonzalez, E. R.; Srinivasan, S. *Electrochim. Acta* **1983**, *28*, 691.

(29) Kadiri, F. E.; Faure, R.; Durand, R. *J. Electroanal. Chem.* **1991**, *301*, 177.

(30) Sasaki, K.; Mo, Y.; Wang, J. X.; Balasubramanian, M.; Uribe, F.; McBreen, J.; Adžić, R. R. *Electrochim. Acta* **2003**, *48*, 3841.

(31) Tammeveski, K.; Arulepp, M.; Tenno, T.; Ferrater, C.; Claret, J. *Electrochim. Acta* **1997**, *42*, 2961.

(32) Kinoshita, K.; Stonehart, P. *Electrochim. Acta* **1975**, *20*, 101.

(33) Kinoshita, K.; Ferries, D. R.; Stonehart, P. *Electrochim. Acta* **1978**, *23*, 45.

(34) Zinola, C. F.; Luna, A. M. C.; Triaca, W. E.; Arvia, A. J. *Electrochim. Acta* **1994**, *39*, 1627.

(35) Perez, J.; Villullas, H. M.; Gonzalez, E. R. *J. Electroanal. Chem.* **1997**, *435*, 179.

(36) Marković, N. M.; Adžić, R. R.; Cahan, B. D.; Yeager, E. B. *J. Electroanal. Chem.* **1994**, *377*, 249.

(37) Toda, T.; Igarashi, H.; Watanabe, M. *J. Electroanal. Chem.* **1999**, *460*, 258.

(38) Marković, N. M.; Gasteiger, H. A.; Ross, P. N. *J. Phys. Chem.* **1995**, *99*, 3411.

(39) Marković, N. M.; Gasteiger, H. A.; Ross, P. N. *J. Phys. Chem.* **1996**, *100*, 6715.

(40) Wang, J. X.; Marković, N. M.; Adžić, R. R. *J. Phys. Chem. B* **2004**, *108*, 4127.

(41) Zhang, J.; Mo, Y.; Vukmirovic, M. B.; Klie, R.; Sasaki, K.; Adžić, R. R. *J. Phys. Chem. B* **2004**, *108*, 10955.

(42) Stamenković, V.; Schmidt, T. J.; Ross, P. N.; Marković, N. M. *J. Phys. Chem. B* **2002**, *106*, 11970.

(43) Igarashi, H.; Fujino, T.; Zhu, Y.; Uchida, H.; Watanabe, M. *Phys. Chem. Chem. Phys.* **2001**, *3*, 306.

(44) Ruban, A.; Hammer, B.; Stoltze, P.; Skriver, H. L.; Nørskov, J. K. *J. Mol. Catal. A* **1997**, *115*, 421.

(45) Toda, T.; Igarashi, H.; Uchida, H.; Watanabe, M. *J. Electrochem. Soc.* **1999**, *146*, 3750.

(46) Toda, T.; Igarashi, H.; Watanabe, M. *J. Electrochem. Soc.* **1998**, *145*, 4185.

(47) Paulus, U. A.; Wokaun, A.; Scherer, G. G.; Schmidt, T. J.; Stamenković, V.; Marković, N. M.; Ross, P. N. *Electrochim. Acta* **2002**, *47*, 3787.

(48) Bard, A. J.; Faulkner, L. R. *Electrochemical Methods*, 2nd ed.; John Wiley & Sons: New York, 2001.

(49) Norton, J. D.; White, H. S.; Feldberg, S. W. *J. Phys. Chem.* **1990**, *94*, 6772.